J Mater Sci (2015) 50:4342–4347
DOI 10.1007/s10853-015-8986-0

Electrospinning-induced preferred dipole orientation in PVDF fibers

Tingping Lei[1] · Lingke Yu[2] · Gaofeng Zheng[2] · Lingyun Wang[2] · Dezhi Wu[2,3] · Daoheng Sun[2]

Received: 25 October 2014 / Accepted: 20 March 2015 / Published online: 9 April 2015

Abstract Polyvinylidene fluoride (PVDF) can be made electroactive by properly mechanical stretching and electric poling treatments of its film, which may be easily realized by single-step electrospinning. This technique is acknowledged as an effective approach to induce rich ferroelectric β-phase in electrospun PVDF fibers; however, the investigation of dipole arrangement during the electrospinning process is still lacking. Here, the piezoelectricity of β-PVDF fibers by electrospinning and forcespinning, a mechanical spinning process without static electric field bias, has been demonstrated. Results show that the electrospun fibers can generate piezoelectric voltage after deformation, while the forcespun fibers nearly show no piezoelectricity for the same condition, revealing that electric field during the electrospinning process can perform in situ poling effect and therefore induces preferred dipole orientation in electrospun PVDF fibers. Further experiments performed in this work show that piezoelectricity of the electrospun fibers increases with increasing fraction of β-phase and/or the applied electric field strength of electrospinning, which provides good guideline for preparing high-performance piezoelectric fibers.

Introduction

Since the discovery of strong piezoelectric activity in polyvinylidene fluoride (PVDF), intensive investigations have been conducted on this polymer. It has at least four different polymorphs referred to as α-, β-, γ-, and δ-phases depending on the processing conditions [1]. Among them, the ferroelectric β-phase shows high piezoelectricity much larger than the other phases, leading to numerous works aiming for high-level β-phase during the past 40 years. A variety of experimental techniques, such as mechanical stretching of the conventionally prepared films and incorporating some additives (e.g., nanoparticles/nanoclays, metal, and metal halides) into PVDF matrix, have been investigated to induce the formation of β-phase [2–5]. For piezoelectric applications, these β-crystal films must be subject to a poling procedure to orient the CF_2 dipoles; however, they are more prone to breakdown under a high-electric field [6].

Recent advances in the electrospinning process provide the possibility of in situ mechanical stretching and electric poling to produce electroactive β-PVDF nanofibers from its polymer solution. A considerable number of studies have reported flexible, high-output piezoelectric nanogenerators based on PVDF fibers using near-field electrospinning (NFES) or conventional far-field electrospinning (FFES) processes [7–11], however, showing conflicting results from FFES research. Some works have shown that electrospun PVDF fibers by FFES can be used directly to prepare a piezoelectric power generator without any extra poling

Electronic supplementary material The online version of this article (doi:10.1007/s10853-015-8986-0) contains supplementary material, which is available to authorized users.

✉ Daoheng Sun
sundh@xmu.edu.cn

[1] Department of Mechanical and Electrical Engineering, Huaqiao University, Xiamen 361021, China

[2] Department of Mechanical and Electrical Engineering, Xiamen University, Xiamen 361005, China

[3] Shenzhen Research Institute of Xiamen University, Shenzhen 518057, China

treatment [10, 11], contradicting results obtained by other authors who have found that the aligned PVDF nanofibers by FFES required a post-poling treatment to make the molecular dipoles oriented along the fiber length direction [9]. The latter one is also supported by Farrar et al., who state that electrospinning fails to induce dipole orientation, because the stretching force and electric field during this process are in the same direction [12]. Despite this, Mandal et al. have observed the preferential orientation of CF_2 dipoles induced in electrospun poly (vinylidene fluoride-trifluoroethylene) [P(VDF-TrFE)] nanofibers by polarized Fourier transform infrared (FTIR) spectroscopy and by detecting the piezoelectric signal from the electrospun nanofiber mat [13]. This orientation is also indicated in recent works reported by Persano et al., where they have developed high-performance piezoelectric devices based on aligned arrays of electrospun P(VDF-TrFE) nanofibers even without any post-poling treatment [14, 15]. However, experimental evidence to elucidate the preferential orientation of dipoles during electrospinning of neat PVDF has not been given yet.

In the present work, piezoelectricity of the ferroelectric β-phase PVDF fibers both by FFES and by forcespinning (only mechanical stretching without electrostatic force) is investigated. Through comparing piezoelectric response of randomly distributed and aligned electrospun fibers with that of forcespun fibers, the dipole orientation of the polymer during electrospinning process is qualitatively determined.

Experimental

Preparation of PVDF fibers

The randomly distributed electrospun and forcespun fibers were obtained by a standard electrospinning apparatus and by a centrifugal device based on a high-speed bench drill, respectively [16, 17]. On the other hand, the aligned electrospun fibers were prepared by replacing a flat-plate collector with a rotating mandrel during the electrospinning process. Based on our recent works [17, 18], polymer solutions of 16 wt% were prepared by dissolving PVDF ($M_w \sim 534{,}000$) powders in *N*-methyl-2-pyrrolidinone (NMP) and acetone with different volume ratios ($V_{NMP}/V_{acetone}$) at 2/8, 3/7, 4/6, 5/5, and 6/4. Specifically, the 'baseline' polymer solution (16 wt%, $V_{NMP}/V_{acetone} = 5/5$) was selected for making forcespun fibers and aligned electrospun fibers, whereas the solutions of 16 wt% with $V_{NMP}/V_{acetone} = 2/8$, 3/7, 4/6, 5/5, and 6/4 were used for producing randomly distributed electrospun fibers. All experiments were performed at room temperature with relative humidity between 55 and 60 %.

Characterization

The surface morphology of electrospun and forcespun fibers was examined using scanning electron microscopes (SEM, LEO 1530 and XL 30) and the fiber diameter was measured from SEM images using ImageJ (available in supporting information). Infrared spectra of the above fiber mats were recorded on a Fourier transform infrared spectrometer (FTIR, Nicolet Avatar 360) in the range of 400–1300 cm^{-1}, with a resolution of 2 cm^{-1}. The relative fraction of β-phase present in each sample was estimated by the Lambert–Beer law, and the characteristic absorption bands at 762 and 840 cm^{-1} corresponding to α- and β-phases, respectively, were used [17, 19]. XRD patterns were collected with an X-ray diffractometer (X'pert PRO, Panalytical) with Cu-K_α radiation ($\lambda = 1.54$ Å) operated at 40 kV and 30 mA. The samples were scanned in the 2θ range from 10° to 40° with a step interval of 0.0167°.

Piezoelectric test of fiber mats

Unlike previously described method [20], a dynamic air pressure test system (Fig. 1) was introduced to measure piezoelectric response of fiber mats. The system mainly consists of a fiber-based pressure sensor, an oscilloscope, a controllable solenoid valve, and a commercially available pressure gage. To better pick up piezoelectric signal generated from the sensor, a signal conditioning circuit was embedded in the stainless steel container, which keeps environmental disturbances (e.g., 50 Hz noise) to a minimum. As for PVDF pressure sensor, two aluminum tapes (diameter: 1.8 cm, thickness: 100 μm) were adhered to the top and the bottom surfaces of the whole fiber mat (thickness around 20 μm), respectively. Two wires were then mounted on the edge of the tapes to ensure appropriate connectivity between the sensor and the signal conditioning unit. Finally, the whole sandwich structure (top electrode, fiber mat, bottom electrode) together with the wires was encapsulated into half-truncated cylinder filled with PDMS of desired shape already and reinforced by casting another PDMS around, as shown in Fig. 1 inset. Application of pressure on the sensor would deform PVDF fiber mat, which may generate piezoelectric potential on the electrodes due to piezoelectric effect. This signal was transmitted to signal conditioning unit and finally recorded on the oscilloscope. Preliminary experimental data demonstrated that the above device showed a relatively

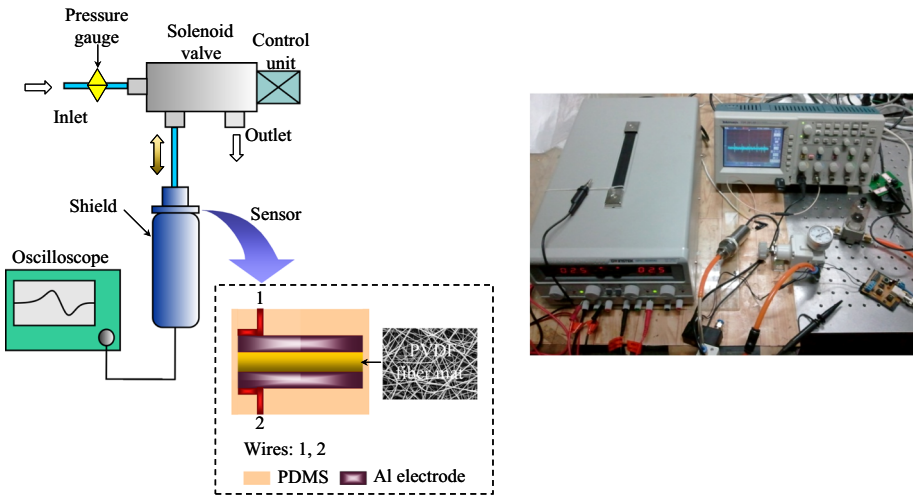

Fig. 1 Schematic illustration (*left*) and the corresponding photo (*right*) of dynamic air pressure test system

good stability during cycling test (Fig. S1 in supporting information) and caused very little damage on the fiber mats (Fig. S2 in supporting information).

Results and discussion

Morphology and polymorphism of electrospun and forcespun fibers

The resulting fibers from the 'baseline' polymer solution (16 wt%, $V_{NMP}/V_{acetone} = 5/5$) by electrospinning and forcespinning are shown in Fig. 2a, b and c, respectively. The electrospun fibers are finer and more uniform than the forcespun fibers. By replacing a static flat-plate collector with a rotating collector, the fibers are well aligned as shown in Fig. 2b. The corresponding XRD patterns and IR spectra of these fiber mats are demonstrated in Fig. 2d and e, respectively. A very strong diffraction peak at $2\theta = 20.6°$ and a weak peak at $2\theta = 36.5°$ corresponding to 110/200 and 020 reflections of the orthorhombic β-phase crystal, respectively, are clearly observed in both electrospun and forcespun fiber mats, as shown in Fig. 2d, indicating the presence of the ferroelectric β-phase [17, 21, 22]. Meanwhile, the characteristic absorption bands of β-phase at 475, 510, 840, and 1275 cm^{-1} are also observed in Fig. 2e [17, 23, 24]. The maximum fractions of β-phase, $F(\beta)_{max}$, for electrospun and forcespun samples are approximately 99 and 95 %, respectively.

Piezoelectricity of electrospun and forcespun fibers

Figure 3a presents piezoelectric output voltage of the above packaged fiber mats under continuous input pressure of 0.2 MPa at a constant frequency of 3 Hz. The maximal output voltage of randomly electrospun fiber mat is nearly

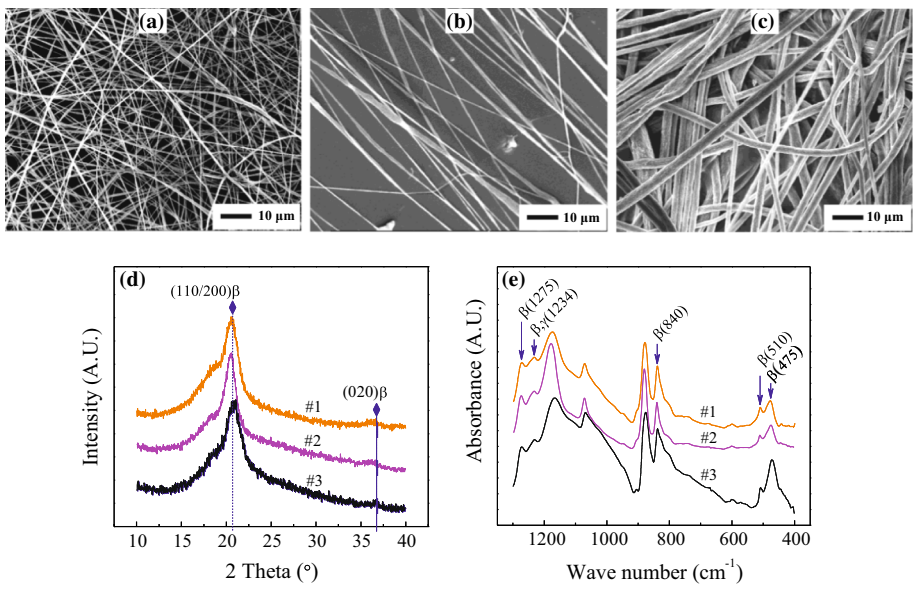

Fig. 2 SEM images of electrospun fibers (**a**) and (**b**) and forcespun fibers at 11000 rpm (**c**); XRD patterns (**d**) and infrared spectra (**e**) of the above fibers. Processing conditions of FFES: applied voltage at 7.5 kV, flow rate at 60 μL h^{-1}, tip-to-collector distance at 10 cm, and rotating speed at 800 rpm for aligned fibers. #1 (*orange*), #2 (*magenta*), and #3 (*black*) in (**d**–**e**) correspond to randomly distributed electrospun fibers (**a**), aligned electrospun fibers (**b**), and forcespun fibers (**c**), respectively (Color figure online)

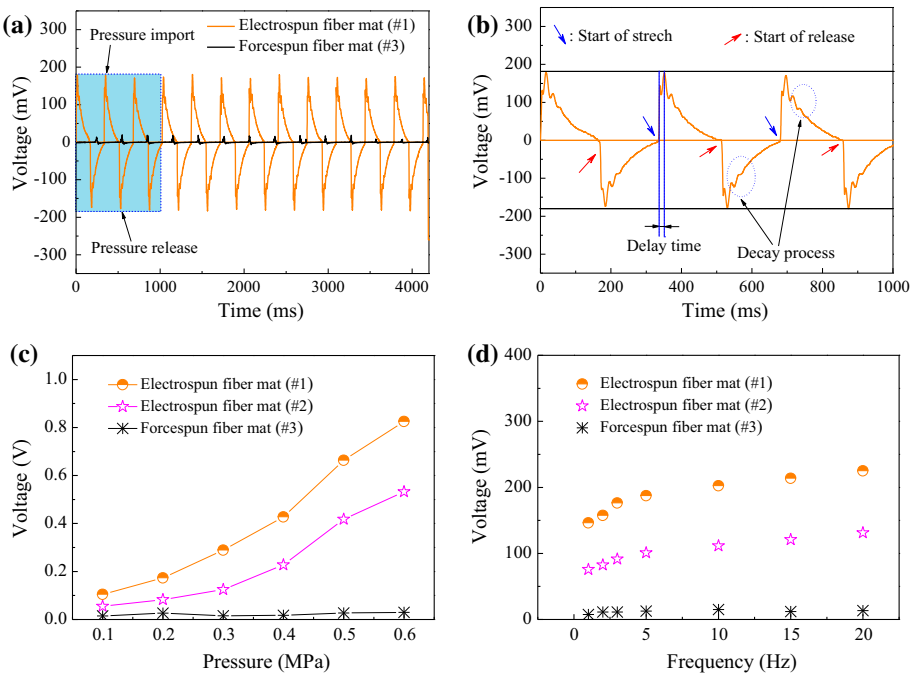

Fig. 3 **a** Piezoelectric output voltages of the above untreated fiber mats under continuous input pressure of 0.2 MPa at a constant frequency of 3 Hz and **b** enlarged picture of the first 1000 ms piezoelectric response of electrospun fiber mats; maximal piezoelectric output voltage of electrospun and forcespun fiber mats subject to **c** different pressures of 0.1–0.6 MPa and **d** different frequencies of 3–20 Hz. The frequency for (**c**) and pressure for (**d**) are 3 Hz and 0.2 MPa, respectively

175 mV, whereas the aligned electrospun fiber mat shows a comparatively low voltage around 83 mV (Figure not shown here), and the forcespun fiber mat only exhibit a very low voltage (~7 mV). Meanwhile, there always appear delay time and decay process during the whole measurement, which can be more clearly observed in Fig. 3b.

To further demonstrate the above difference from electrospun and forcespun fiber mats, they were subjected to different pressure magnitudes and frequencies for piezoelectric measurement. As can be seen in Fig. 3c, with increasing pressure magnitude, the maximal output voltage for electrospun samples rises proportionally but makes no difference (still very low) for forcespun samples. It is apparent that inletting more pressure causes greater deformation in the mats, which can induce more piezoelectric bound charges (polarization); as a result, an increase in output voltage is observed in the electrospun samples [7]. Likewise, the maximal piezoelectric output voltage of electrospun samples increases with the frequency of airflow but becomes steady afterwards (Fig. 3d). It may be attributed to the shortening interval between the delay and the decay processes and/or better impedance matching with the measurement system due to increase in the frequency [7, 25], which results in higher piezoelectric voltage outputs in piezoelectric electrospun β-phase fiber mats.

Effect of $F(\beta)$ and electric field strength on piezoelectricity of electrospun fibers

To demonstrate the effect of $F(\beta)$ on piezoelectricity of electrospun fibers, samples electrospun from 16 wt% solutions of $V_{NMP}/V_{acetone}$ = 2/8, 3/7, 4/6, and 6/4 are also experimented (their morphologies available in Fig. S3 in supporting information). IR spectra demonstrated that samples from 16 wt% solutions of $V_{NMP}/V_{acetone}$ from 2/8 to 6/4 are all β-rich, with an average $F(\beta)$ greater than 95 % (Fig. S4 in supporting information). Figure 4a shows the piezoelectricity of samples with $F(\beta)$ ranging from 95 to 99 % under the aforementioned measurement condition. With increasing $F(\beta)$, the output voltage is increased accordingly. It has been reported that poled samples with higher fraction of β-phase show higher d_{33} piezoelectric coefficients [26], and therefore probably exhibit higher voltages. However, it should be noted that the piezoelectric performance of PVDF fibers is affected by both the fraction of β-phase and the total dipole moment (closely related to the poling effect). Hence, the following is to investigate the effect of applied electric field on piezoelectricity of electrospun fibers.

We found that electrospun samples from the 'baseline' polymer solution (16 wt%, $V_{NMP}/V_{acetone}$ = 5/5) by only varying the applied voltage from 4 to 11 kV have good morphology and high-β-phase concentration, $F(\beta) \geq 95$ % (Figs. S5 and S6 in supporting information). Figure 4 shows maximum piezoelectric outputs of eight typical samples (without experiencing any post-poling procedure), which almost have the same $F(\beta)$ and thickness of around 95 % and 20 μm, respectively. With increasing the voltage from 4 to 11 kV, the output voltage first goes up steadily but very slowly until the applied voltage reaches a critical value of 10 kV. Generally, an electric poling field of nearly 10^7 V m^{-1} and a first-rising-up and then lowering down to

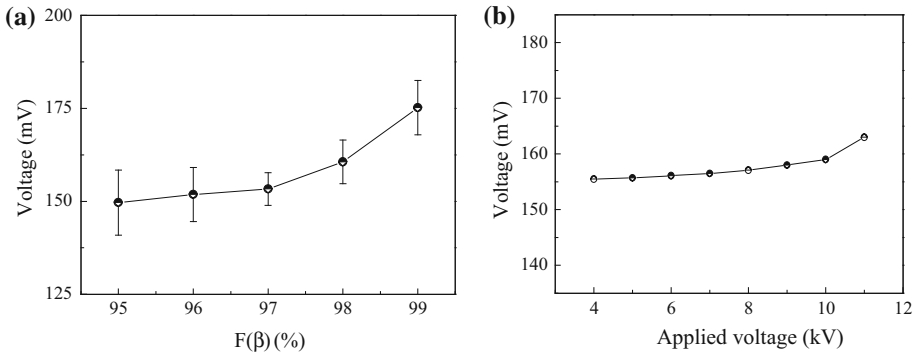

Fig. 4 **a** Piezoelectric output voltages of electrospun fibers produced from 16 wt% PVDF solutions, with NMP and acetone ratios ($V_{NMP}/V_{acetone}$) at 2/8, 3/7, 4/6, 5/5, and 6/4; **b** piezoelectric output voltage of electrospun fibers produced from the 'baseline' system (16 wt%, $V_{NMP}/V_{acetone}$ = 5/5) by only varying the applied voltage from 4 to 11 kV. All the above samples are measured under continuous input pressure of 0.2 MPa at a constant frequency of 3 Hz

room temperature are required to give an effective poling effect on the stretched β-phase PVDF films [27]. As for room-temperature electrospinning, the high-static electric field applied during this process, in a manner, can simultaneously stretch PVDF molecules and orient the CF_2 dipoles effectively [28], although the electric field strength of FFES is far behind ($\sim 10^5$ V m^{-1}).

From the above results, it is clear that PVDF fiber samples produced by forcespinning are nonpiezoelectric although with high fraction of β-phase. In the process of forcespinning, the fibers are produced by centrifugal force instead of electrostatic force to eject the polymer solution. As such, the polymer jet just undergoes the stretching process, a procedure similar to the uniaxial stretching process performed on PVDF films, hence only inducing α → β phase transformation in randomly distributed fibers [29]. Although the unit cell of the β-form crystal of PVDF has a permanent dipole, in the case of stretching-only samples, the direction of dipole vectors and/or polarization of individual crystallites may be random about the drawing axis, and hence, the specimen may have no net polarization, as illustrated in Fig. 5 (left). Therefore, no visible piezoelectric activity was observed in the forcespun β-PVDF fibers, since the piezoelectricity appears only when the crystallites have a preferred orientation.

In this respect, electrospinning is preferable because of the high-static electric field applied during this process [28]. Reneker and Yarin reported that in the FFES process, the typical path of the jet is a shortly straight segment followed by a coil of increasing diameter (see right top in Fig. 5), and the trajectory of each short segment of the coil is almost perpendicular to the electric field [30]. It is therefore reasonable to propose that the electric field during this process can carry out poling effect on the stretching polymer jet, although the resulting electric poling field (~ 1 kV cm^{-1}) from the FFES process is much lower than the post-poling field (~ 300 kV cm^{-1}) applied on the stretched films [27]. As illustrated in Fig. 5 (right), the induced oriented CF_2 dipoles are along the z axis (the mat thickness direction), i.e., polarization of crystallites has a preferential orientation along this axis, and the resultant polarization appears. Hence, a macroscopic piezoelectricity was normally observed in the electrospun β-PVDF fibers.

Conclusions

We have ascertained a way to prove the preferential orientation of the dipoles in the electrospun PVDF fibers by comparing macroscopic piezoelectricities of high-fraction

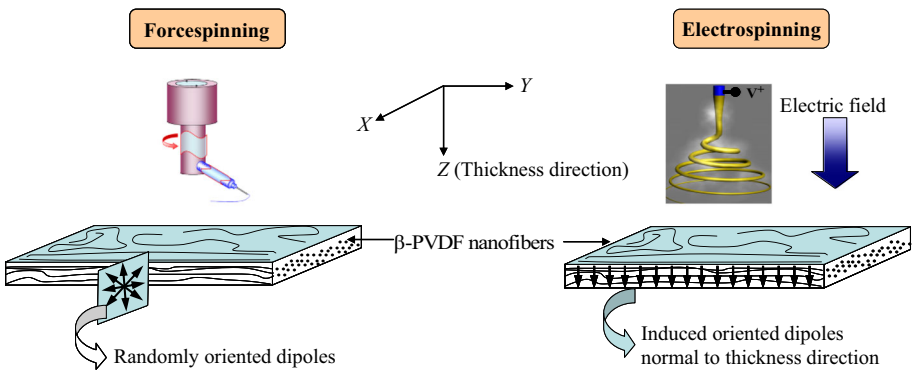

Fig. 5 Schematic representation of the dipole arrangement in the fiber mats produced by forcespinning (*left*) and electrospinning (*right*)

β-PVDF fibers both produced by electrospinning and forcespinning. Results showed that the electrospun sample was piezoelectricity active and its piezoelectric output voltage can be enhanced by increasing pressure magnitude and/or airflow frequency, while the forcespun sample nearly showed no piezoelectricity at all time. Further experiments on some key parameters revealed that piezoelectricity of electrospun samples themselves was increased with increasing β-phase concentration and/or the applied electric field strength. Finally, a simplified process for dipole arrangement during the electrospinning and forcespinning processes was depicted.

Acknowledgements The authors thank Nanotechnology Center of Xiamen University for the SEM work, and Mrs. Xinyu Liu and Mr. Yiwen Ye at Xiamen University for IR and XRD measurements, respectively. This work was supported by the National Natural Science Foundation for Youth of China (No. 51105320), the National Natural Science Foundation of China (No. 51305373), and Science and Technology Program of Shenzhen City (No. JCYJ2012 0615161609592).

References

1. Sessler G (1981) Piezoelectricity in polyvinylidenefluoride. J Acoust Soc Am 70:1596–1608
2. Sajkiewicz P, Wasiak A, Goclowski Z (1999) Phase transitions during stretching of poly (vinylidene fluoride). Eur Polym J 35:423–429
3. Dang ZM, Lin YH, Nan CW (2003) Novel ferroelectric polymer composites with high dielectric constants. Adv Mater 15: 1625–1629
4. Yoon S, Prabu A, Kim K, Park C (2008) Metal salt-induced ferroelectric crystalline phase in poly (vinylidene fluoride) films. Macromol Rapid Commun 29:1316–1321
5. Yu L, Cebe P (2009) Crystal polymorphism in electrospun composite nanofibers of poly (vinylidene fluoride) with nanoclay. Polymer 50:2133–2141
6. Sakata J, Mochizuki M (1991) Preparation of organic thin films by an electrospray technique I. Crystal forms and their orientation in poly (vinylidene flouride) films. Thin Solid Films 195:175–184
7. Chang C, Tran VH, Wang J, Fuh Y-K, Lin L (2010) Direct-write piezoelectric polymeric nanogenerator with high energy conversion efficiency. Nano Lett 10:726–731
8. Liu Z, Pan C, Lin L, Huang J, Ou Z (2014) Direct-write PVDF nonwoven fiber fabric energy harvesters via the hollow cylindrical near-field electrospinning process. Smart Mater Struct 23:025003
9. Hansen BJ, Liu Y, Yang R, Wang ZL (2010) Hybrid nanogenerator for concurrently harvesting biomechanical and biochemical energy. ACS Nano 4:3647–3652
10. Fang J, Wang X, Lin T (2011) Electrical power generator from randomly oriented electrospun poly (vinylidene fluoride) nanofibre membranes. J Mater Chem 21:11088–11091
11. Yu H, Huang T, Lu M et al (2013) Enhanced power output of an electrospun PVDF/MWCNTs-based nanogenerator by tuning its conductivity. Nanotechnology 24:405401
12. Farrar D, Ren K, Cheng D et al (2011) Permanent polarity and piezoelectricity of electrospun α-helical poly (α-amino acid) fibers. Adv Mater 23:3954–3958
13. Mandal D, Yoon S, Kim KJ (2011) Origin of piezoelectricity in an electrospun poly (vinylidene fluoride-trifluoroethylene) nanofiber web-based nanogenerator and nano-pressure sensor. Macromol Rapid Commun 32:831–837
14. Persano L, Dagdeviren C, Su Y et al (2013) High performance piezoelectric devices based on aligned arrays of nanofibers of poly (vinylidenefluoride-co-trifluoroethylene). Nat Commun 4:1633
15. Persano L, Dagdeviren C, Maruccio C, De Lorenzis L, Pisignano D (2014) Cooperativity in the enhanced piezoelectric response of polymer nanowires. Adv Mater 26:7574–7580
16. Lei T, Zhan Z, Zuo W et al (2012) Electrospinning PVDF/EC fibre from a binary solvent system. Int J Nanomanuf 8:294–305
17. Lei T, Cai X, Wang X et al (2013) Spectroscopic evidence for a high fraction of ferroelectric phase induced in electrospun polyvinylidene fluoride fibers. RSC Adv 3:24952–24958
18. Lei T, Yu L, Yang F, Sun D (2015) Predicting polymorphism of electrospun polyvinylidene fluoride membranes by their morphologies. J Macromol Sci Part B 54:91–101
19. Gregorio R Jr, Cestari M (1994) Effect of crystallization temperature on the crystalline phase content and morphology of poly (vinylidene fluoride). J Polym Sci Part B 32:859–870
20. Lei T, Xu L, Zhan Z et al (2011) Direct fabrication of polymer nanofiber membrane for piezoelectric vibration sensor. In: Sensors, 2011 IEEE, Limerick, pp 1367–1370
21. Hasegawa R, Takahashi Y, Chatani Y, Tadokoro H (1972) Crystal structures of three crystalline forms of poly (vinylidene fluoride). Polym J 3:600–610
22. Esterly D, Love B (2004) Phase transformation to β-poly (vinylidene fluoride) by milling. J Polym Sci Part B 42:91–97
23. Kobayashi M, Tashiro K, Tadokoro H (1975) Molecular vibrations of three crystal forms of poly (vinylidene fluoride). Macromolecules 8:158–171
24. Boccaccio T, Bottino A, Capannelli G, Piaggio P (2002) Characterization of PVDF membranes by vibrational spectroscopy. J Membr Sci 210:315–329
25. Zheng G, Wang X, Li W et al (2011) Single-step fabrication of organic nanofibrous membrane for piezoelectric vibration sensor. In Solid-state sensors, actuators and microsystems conference (TRANSDUCERS), 16th international, pp 2782–2785
26. Gomes J, Nunes JS, Sencadas V, Lanceros-Méndez S (2010) Influence of the β-phase content and degree of crystallinity on the piezo-and ferroelectric properties of poly (vinylidene fluoride). Smart Mater Struct 19:065010
27. Kawai H (1969) The piezoelectricity of poly (vinylidene fluoride). Jpn J Appl Phys 8:975–976
28. Kaura T, Nath R, Perlman M (1991) Simultaneous stretching and corona poling of PVDF films. J Phys D Appl Phys 24:1848–1852
29. Salimi A, Yousefi A (2003) Analysis Method: FTIR studies of [beta]-phase crystal formation in stretched PVDF films. Polym Test 22:699–704
30. Reneker DH, Yarin AL (2008) Electrospinning jets and polymer nanofibers. Polymer 49:2387–2425